Dispensing particles under atmospheric and vacuum conditions using an electrostatic device

Jon B. Olansen[a] and Patrick F. Dunn[b]
Department of Aerospace & Mechanical Engineering, University of Notre Dame, Notre Dame, Indiana 46556

Vincent J. Novick
Engineering Physics Division, Argonne National Laboratory, Argonne, Illinois 60439

(Received 14 June 1989; accepted for publication 29 August 1989)

Experiments were conducted to determine the operational characteristics of an electrostatic device that dispenses micrometer-size particles continuously without the use of a carrier gas. The dispenser's operational performance was determined under different operating conditions based upon four independent experimental variables: the environmental pressure in which the dispenser was operated, its interelectrode spacing, the applied voltage, and the type of particle used. Measurements were made of the dispenser's operating current and voltage, particle mass dispensing efficiency, and dispensed particle mass flow rate, current, and velocity. An increase in the strength of the dispenser's internal electric field was found to produce an increase in operating current and dispensed particle velocity, current, and mass flow rate. The measured average charge acquired by a particle and the particle average velocity under vacuum conditions were predicted using single particle theory. All temporal measurements of the dispensed particle mass were correlated nondimensionally, independent of the particle type, interelectrode spacing, and applied voltage. The dispensing efficiency under atmospheric conditions, when expressed as a function of the strength of the internal electric field above the minimum field required for particle levitation against gravity, was shown to be independent of particle type.

I. INTRODUCTION

This paper presents the results of experiments and analytical studies conducted to characterize the operational performance of a laboratory-scale electrostatic powder dispenser (EPD). This device continuously dispenses solid, micrometer-size particles at a high efficiency under either atmospheric or vacuum conditions without the use of a carrier gas or any mechanically moving parts. There are many potential applications for such a device, from the terrestrial applications of electrostatically controlled particle igniters (Yu and Colver[1]), laboratory particle generators for calibration and testing, and particle transport devices, to the space applications of hypervelocity particle accelerators (Shelton, Hendricks, and Wuerker[2]), material transporters, and low-level thrusters.

This means of particle generation is based upon the principles of electrostatic particle levitation and transport. Benjamin[3] reported the first use of these processes by Andrew Gordon in 1742 to produce the chiming of bells. Benjamin Franklin[4] later used this chiming technique to detect the presence of electrified clouds associated with thunderstorms. It was not until 200 years later, however, that detailed studies were undertaken to analyze the physical mechanisms behind these phenomena.

Studies conducted within the past 30 years specifically have been related to particle electrostatic charging, removal from surfaces, and transport. The contact charging of spherical, micrometer-size (0.3–15 μm diameter), conducting, semiconducting, and dielectric particles has been experimentally investigated by Cho.[5] Colver[6] reported the results of analytical and experimental studies on the electrical charging of dielectric and metallic micrometer-size (29–4760 μm diameter) particles while in stationary or dynamic contact with a charged wall.

Myazdrikov and Puzanov[7] have conducted experiments on the effect of surface adhesion on the electrostatic removal of particles from surfaces, whereas Cooper, Wolfe, and Miller[8] and Cooper and Wolfe[9] have studied, analytically and experimentally, the electrostatic removal of particle singlets and doublets from conductive surfaces. Most recently, Novick, Hummer, and Dunn[10] have reported the results of experiments and an analytical model for the electrostatic removal of micrometer-size particles from a layer of particles residing on a conductive surface.

The electrostatic dispersion of particles at hypervelocities of the order of km/s has been studied by Shelton, Hendricks, and Wuerker.[2] Adamo and Nanevicz[11] were the first to develop an electrostatic device capable of continuously dispensing bulk powder as micrometer-size particles in a vacuum. More recently, Olansen[12] has conducted experiments to characterize the operational performance of an EPD, the design of which was adapted from that of Adamo and Nanevicz.[11]

These studies indicate that the parameters that significantly affect the dispenser's operational performance are the environmental pressure in which the dispenser is operated, its interelectrode spacing and applied voltage (hence, its internal electric field strength) and the diameter and density of

[a] Present address: Rockwell Space Operations Co., DF43, NASA/JSC, Houston, TX 77058.
[b] To whom all correspondence should be addressed.

 0021-8979/89/246098-12$02.40

the particles are used. These factors dominate when particles with diameters greater than approximately 10 μm are dispensed electrostatically, where the adhesion force between the particles and their initial residing surface is negligible.

The primary purposes of this paper are to describe the operational performance of the EPD in terms of these parameters and to ascertain the utility of single-particle theory in predicting the experimental results. This paper correlates measurements of the dispenser's operating current and voltage, dispensing efficiency, and dispensed particle mass flow rate, current, and velocity as a function of environmental pressure, interelectrode spacing of the dispenser, applied voltage, and particle diameter and density. Where appropriate, these results are nondimensionalized or evaluated in terms of theory. The results reported herein are the first in the literature on the operational characteristics of a device of this nature.

II. THEORETICAL BACKGROUND

The design and operation of an electrostatic powder dispenser as shown in Fig. 1 is based upon the principles of the electrostatic levitation and transport of particles. In this device, powder is placed upon (or continually supplied to) the top of its center electrode. A potential difference is applied between the center and outer (electrically grounded) electrodes, thereby establishing an internal electric field. A charge on the particles residing on the center electrode is acquired by induction. If the field strength is sufficient, the particles are removed from the center copper electrode and travel to the upper, outer electrode. Upon reaching this electrode, an opposite charge is induced on the particles and they subsequently travel back to the center electrode. The upper electrode is shaped so that as this process repeats itself, the particles traverse radially outward until they eventually pass through the screen into the lower chamber. After doing so, the particles are focused over the exit orifice by the shape of the lower electrode and are subsequently dispensed from the device. The slanted configurations of the upper and lower stainless-steel electrodes produce a nonuniform electric field that focuses the particles over the screen and eventually the exit orifice.

A goal of this study is to develop an analytical model for this device that relates the device's operating characteristics to its design and operating parameters. Specifically, a successful model would relate the minimum electric field required initially to levitate the particles, the particle charge and velocity, total particle current and power required for steady-state operation to the environmental pressure in which the dispenser was operated, its interelectrode spacing and applied voltage, and the type of particle used.

At present, it is difficult to develop such a model, primarily because of the complexity introduced by the multiply oriented electrode surfaces and internal electric field inside the device. To date, the theory describing the operational performance of such a device has geen given only in terms of the steady-state behavior of a single particle within a parallel-plate capacitor geometry (Adamo and Nanevicz,[11] Cho,[5] and Colver[6]). This single-particle theory approach, however, has been sufficient to describe many of the experimental results of these studies within reasonable agreement.

Single-particle theory is a good approximation to actual particle behavior inside an EPD for several reasons. First, all of the significant governing parameters are considered in the theory. Second, the internal electrode walls of an EPD are nearly parallel, which is assumed in the theory. Finally, typical particle number concentrations inside an EPD are on the order of $10^3/\text{cm}^3$ (depending on particle size), and the "mean free path" of a particle traveling inside an EPD under typical operating conditions is on the order of the spacing between the electrodes. Consequently, the number of particle–particle collisions inside the device are negligible, which also is assumed in the theory.

For a single particle in a parallel-plate capacitor arrangement, estimates of the charge that the particle acquires depends upon several assumptions. For the case of a single, conductive particle in a uniform electric field, the total charge induced on the particle as it is separated from contact with a conductive surface is given by (Shelton, Hendricks, and Wuerker,[2] Adamo and Nanevicz,[11] Cho,[5] Myazdrikov and Puzanov[7])

$$q = \pi^3 \epsilon_0 D^2 E/6 = 1.65\pi\epsilon_0 D^2 E, \quad (1)$$

where $E = V/d$, electric field strength (V/m), $D =$ the particle diameter (m), $d =$ the interelectrode spacing (m),

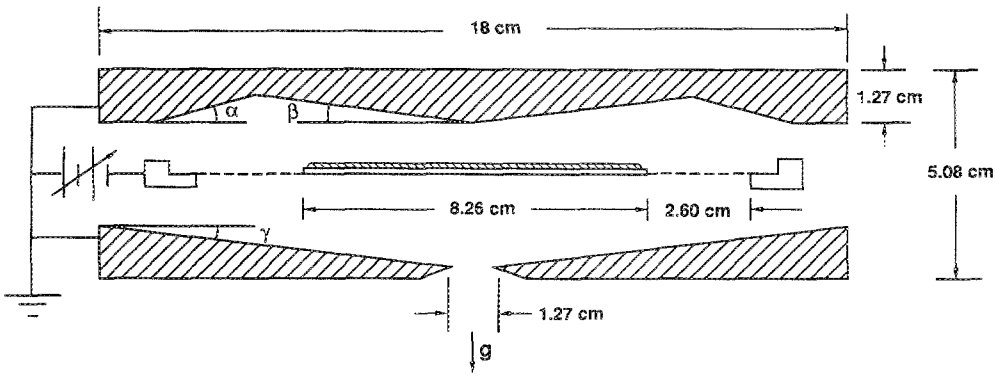

FIG. 1. Schematic of the EPD.

$V=$ the applied voltage (V), and $\epsilon_0 =$ the permittivity of free space (8.85×10^{-12} F/m). This expression for particle charge is useful only in determining the electrostatic force on the particle in a uniform electric field (where $F_e = qE$), not while the particle is residing on a conductive surface. The expression for the charge that a particle can acquire for the case of a single isolated conductive particle residing on an infinite conductive plane is given by (Novick, Hummer, and Dunn[10])

$$q = 1.37\pi\epsilon_0 D^2 E. \tag{2}$$

In order to determine the force required to remove the particle from a conductive surface, it is necessary to consider the effect of the surfaces contacting and adjacent to the particle on its surface charge distribution. Inside an EPD, particle motion will initiate when the particle acquires a charge that is sufficient to levitate itself against gravity and adhesion from the particle reservoir. If the particles are sufficiently large, with diameters greater than approximately 10 μm, particle adhesion may be assumed to be negligible. Consequently, for larger particles, the charge must only be sufficient enough to allow the electrostatic forces to levitate the particle against gravity.

If the particle is surrounded by neighboring particles, the surface charge distribution will be less. Novick, Hummer, and Dunn[11] have shown that a surface charge distribution of approximately one-half of that expected for an isolated particle [given by Eq. (2)] accurately describes and predicts the minimum electric field strength required to levitate the particles in a powder layer against gravity. Their data and analysis show that the minimum electric field strength required to levitate particles is given by

$$E = 5.21\times10^5(\rho D)^{1/2}, \tag{3}$$

where D in their analysis represents the particle mass median diameter.

After levitation, the overall motion of the charged particles produces an electrical current. There are two particle currents that result from two possible current pathways, as shown in Fig. 2. These are the current carried from the EPD by the particles I_p and the current lost to electrical ground inside the EPD I_g because of the charge transfer that occurs during each particle collision with a ground electrode.

With the total number of particles n contained in a mass M of powder with density ρ being

$$n = 6M/\pi D^3\rho, \tag{4}$$

the total charge carried from the EPD by this mass of dispensed powder becomes

$$\begin{aligned} Q = qn &= \pi^2 M\epsilon_0 V/D\rho d \\ &= 8.22M\epsilon_0 V/D\rho d. \end{aligned} \tag{5}$$

In these two equations, it is implicitly assumed that the particle size distribution is monodisperse, where the particle diameter of average area D_{20} and the diameter of average mass D_{30} are denoted by D. If the particle size distribution is polydisperse, then D is replaced in Eq. (4) by the diameter of average mass and in Eq. (5) by the diameter of average area. This yields

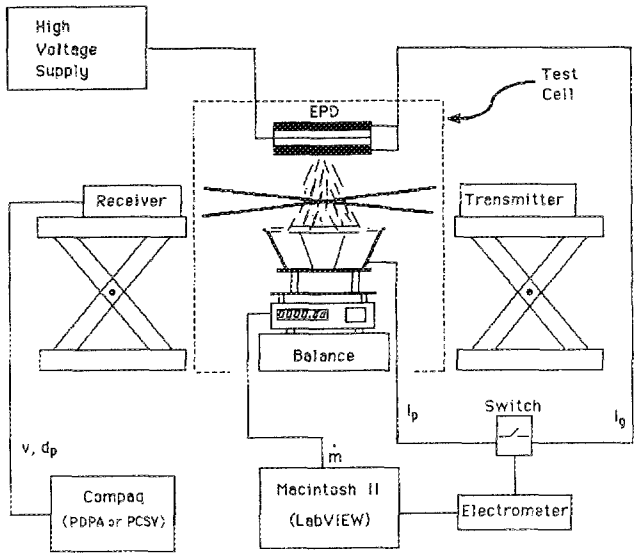

FIG. 2. Schematic of the experimental setup.

$$Q = \left(\frac{8.22M\epsilon_0 V}{\rho d}\right)\left(\frac{D_{20}^2}{D_{30}^3}\right). \tag{6}$$

The current $I_p\,(=Q/t)$ carried from the EPD by the exiting particles becomes

$$I_p = \left(\frac{8.22M\epsilon_0 V}{t\rho d}\right)\left(\frac{D_{20}^2}{D_{30}^3}\right), \tag{7}$$

where t denotes time. Further, if each particle collides N times with the ground electrodes before it exits and there is a charge transfer of $2q$ to a ground electrode during each collision, the ground current can be expressed as

$$I_g = 2QN/t. \tag{8}$$

The average number of total collisions or bounces N, that each particle makes with either electrode before it exits the EPD is determined by dividing the ground current I_g by twice the particle current I_p or

$$N = I_g/2I_p. \tag{9}$$

The factor of 2 is present in Eq. (9) because the ground current represents the charge transfer per collision. This method of determining the number of particle bounces assumes no particle–particle collisions during transit between the electrodes.

Using this information, the power required for steady-state operation of the EPD can be determined. This is given as the product of the applied voltage and total current. Under these conditions, the power required to dispense a mass M of powder can be expressed as

$$P = IV = (I_p + I_g)V = (VQ/t)(1+2N). \tag{10}$$

However, because typically $2N \gg 1$, the total current can be approximated by the ground current, therefore, the power required to dispense a mass of powder becomes

$$P = \left(\frac{16.44M\epsilon_0 V^2 N}{t\rho d}\right)\left(\frac{D_{20}^2}{D_{30}^3}\right). \tag{11}$$

Different expressions for the average velocity v of a particle exiting the EPD can be determined depending upon the environmental pressure in which the EPD is operated. Under vacuum conditions, assuming no particle collisions, the conservation of energy equation for the particle yields

$$v = \left(\frac{2\epsilon_0 \pi^2 V^2}{(D_{30}^3/D_{20}^2)\rho d} + 2gh \right)^{1/2}, \tag{12}$$

where h is the height from the last surface (usually the bottom surface of the center electrode) to the point where the velocity is determined (usually several cm directly below the EPD's exit orifice). This equation can be solved directly for the average particle velocity. Under atmospheric conditions, there is an additional force, a drag force, that acts upon the particles. Thus, Eq. (12) is rewritten to arrive at

$$v = \left(\frac{2\epsilon_0 \pi^2 V^2}{(D_{30}^3/D_{20}^2)\rho d} + 2gh - \frac{12 F_D h}{\pi \rho D_{30}^3} \right)^{1/2}, \tag{13}$$

where F_D is the drag force on the particle. This equation must be solved numerically because the drag force depends upon the particle velocity. A more detailed analysis of these equations is presented by Olansen.[12]

III. EXPERIMENTAL INVESTIGATION

A cross-sectional view of the laboratory-scale EPD used in the present study is shown in Fig. 1. The electrode wall angles α, β, and γ shown in the figure are 10°, 5.4°, and 8.2°, respectively. A schematic of the experimental configuration is shown in Fig. 2.

A potential difference between the center and outer electrodes is achieved by applying a high voltage to the center copper electrode while grounding the two stainless steel outer electrodes. The center electrode consisted of a 2-mm-mesh copper screen supporting a 8.25-cm-diam copper plate upon which the powder initially resided. The stainless-steel electrodes were each 1.27 cm thick at the outer edge. Delrin and plexiglas rings of various thicknesses were used to achieve the variable interelectrode spacings that were required for the present experiments.

As indicated by single-particle theory, the primary variables expected to determine the operational characteristics of the EPD are the particle type, the voltage applied to the EPD, the interelectrode spacing of the EPD, and the environmental pressure in which the EPD was operated. The values of these independent variables used in the present study are presented in Table I.

TABLE I. Experimental independent variables.

Primary materials:
Type 410 stainless steel (10–60 μm)
Type 316 stainless steel (60–125 μm)
Silver-coated hollow glass (10–100 μm)
Interelectrode spacing:
1.27 cm
1.905 cm
2.54 cm
3.175 cm
Applied voltage:
4 voltages per spacing:
1.27-cm spacing 5.0, 6.5, 8.0, 9.5 kV
1.905-cm spacing 7.5, 9.75, 12.0, 14.25 kV
2.54-cm spacing 10.0, 13.0, 16.0, 19.0 kV
3.175-cm spacing 12.5, 16.25, 20.0, 23.75 kV
Operating pressure:
Atmospheric
Vacuum ($<9\times10^{-5}$ Torr)

A number of different materials and particle sizes were used in this study in order to generalize the operational characteristics of the dispenser as much as possible. However, the majority of experiments were conducted using three different particles as noted in Table I. This was because the particle type had to be restricted to spherical particles for velocity measurements using the PDPA system and also because theory suggested a strong dependency on particle size and density. Two types of spherical stainless steel particles [Duke Scientific, Type 410, Catalog No. 435, Lot No. 7791 (10–60 μm diameter) and Type 316, Catalog No. 436, Lot No. 8335 (60–125 μm diameter)] were chosen to elucidate the effect of particle diameter on the EPD performance. Silver-coated hollow glass microspheres [P.A. Industries, Metalite Silver, SF-14 (10–100 μm diameter)] were chosen so that particles similar in size to the stainless steel particles but with a different density could be studied. The additional types of particles, summarized in Table II, with diameters ranging from approximately 10–200 μm, were used in some of the experiments to provide supplementary data.

The majority of atmospheric tests for this research were conducted in an open-air arrangement, whereas several atmospheric and all of the vacuum tests were performed inside of a large stainless-steel vacuum tank. This tank was cylindrical in shape with a 76.2 cm (30 in.) diameter and 152.4 cm (60 in.) length and had a volume of 24.5 cubic feet. A pumping system, consisting of two mechanical roughing pumps (a Heraeus-Englehard Model E-135 and an Edwards Model E2M12) and an Edwards Model 160M Diffstak diffusion pump, was used to produce a vacuum on the order of 10^{-5} Torr.

In order to dispense the particles that were placed inside the EPD on the copper plate, a high voltage on the order of several kV was applied to the center electrode. A Glassman high voltage power supply, Series PH, Model PS/PH050N60-X18, was utilized for this purpose. It provided a continuous adjustable output voltage from 0 to 50 kV at currents up to 60 mA.

The particles that were emitted from the EPD were collected on an electrically isolated plate or pan at least approximately 25 cm below the EPD exit. The plate was connected electrically through a relay switch to a Keithley Model 617 programmable electrometer which measured the current carried from the EPD by the particles. The purpose of the relay switch was to enable the electrometer to read both the effluent particle current described above and the current lost to ground by particle collision with the ground electrodes inside the EPD. For experiments conducted in open air, a copper plate was set on a Sartorius electronic balance, Model E 8100 P, to measure the accumulated particle weight dispensed by the EPD.

The dispensed particle velocity measurements on the

spherical particles listed in Table I were acquired using a phase Doppler particle analyzer (PDPA) designed and manufactured by Aerometrics, Inc. (Bachalo and Houser[13]). The PDPA system operates under the same principle as a typical laser Doppler velocimeter system with one additional feature; it uses three photodetectors instead of one. This enables both the particle diameter and velocity to be determined from the light scattered off of spherical droplets or particles. Because spherical, opaque particles were used in this set of experiments, only the reflected light scattered from the particles was collected. For the open-air tests, the PDPA system was set up to receive light in the 30° forward scatter mode. For the tests conducted in the vacuum tank, the 90° side scatter receiver configuration was utilized.

The dispensed particle velocity measurements on the nonspherical test powders listed in Table II were made using a particle counter-sizer-velocimeter (PCSV) designed and manufactured by Insitec (Holve and Annen[14]). The PCSV is basically a single particle counting system that utilizes one focused laser beam. Absolute particle concentration, size distribution, and speeds are determined from the intensities and widths of the scattered light pulses using an intensity deconvolution algorithm. In this set of experiments, the scattered light was collected 3.6° off axis in the forward scatter mode.

For all of the experiments conducted, the operating parameters and several of the output test variables were monitored using the National Instruments LabVIEW software data acquisition package and a Macintosh II computer. Data were acquired from a serial port and from an IEEE bus port. These ports were used for recording the accumulated effluent particle mass data (via an RS-232 serial port) the dispensed particle, and particle lost-to-ground currents (via an IEEE bus port). Typically, data were acquired at a sample rate of one set per second for a duration from approximately 30–300 s.

The parameters that were measured or determined directly from the measurements described above included the EPD's minimum voltage for particle levitation, its dispensing efficiency and dispensed particle mass flow rate, the particle current carried from the EPD, the particle current lost to ground inside the EPD, the particle average exit velocity, and the EPD's power requirement.

TABLE II. Additional materials.

Particle type	Density (kg/m^3)	Mass median diam (μm)
Silver-coated hollow glass microspheres (Ag SF-44)	850	31.5
Brass microspheres (brass)	9404	135
Copper dust (Cu dust)	9977	12.0
Copper-coated hollow glass microspheres (Cu SG)	825	90
Zinc powder (Zinc)	7140	14.5

IV. RESULTS AND DISCUSSION

The experimental results that characterize the performance of the EPD and its output are described and discussed. First, the results of experiments conducted to determine the minimum voltage required for particle levitation inside the EPD are presented. Second, the experimental results regarding the dispensed particle mass flow rate, dispensed particle current, particle current lost to ground, and dispensed particle velocity as a function of the EPD operating parameters are considered. Finally, experimental results of the dispensing efficiency of the EPD are presented.

A. Minimum threshold voltage

In the first series of experiments, data were obtained to determine the minimum voltage required to levitate particles inside the EPD. Above this minimum threshold voltage, the electrostatic force on the particles in the top layer of the powder bed of the EPD becomes greater than the combined forces of gravity and adhesion. The particles thereby obtain motion towards the upper electrode. Novick, Hummer, and Dunn[11] have reported the functional dependence of the minimum electric field required for levitation on the diameter and density of the particles used. Assuming that the force due to adhesion is negligible, as shown for particles greater than approximately 10 μm in diameter in their study, their particle force balance yielded a minimum applied electric field given by Eq. (3), where the electrostatic force on each particle equaled $0.68\,\pi\epsilon_0 D^2 E^2$.

A plot of the minimum electric field versus $(\rho D)^{1/2}$ for the present experiments obtained under both vacuum and atmospheric conditions using all of the materials listed in Tables I and II is shown in Fig. 3. A least-square fit of this data yielded $E = [0.915 + 3.99(\rho D)^{1/2}] \times 10^5$, which is shown by a dashed line in the figure. These results are consistent with those of Novick, Hummer, and Dunn,[11] where a least-square fit of their data yielded $E = [0.362 + 4.85(\rho D)^{1/2}] \times 10^5$, which is shown by a solid line in the figure. It appears that for the smaller, lower density particles, a somewhat higher electric field strength above that found under vacuum conditions is required when the EPD is operated under atmospheric conditions. This is probably due to the effect of humidity in the air, which can increase particle adhesion. Humidity in the atmospheric cases also contributes to charge leakage from the surface of the particles to ions present in the air. This current leakage was measured to be from 0.01 to 10 μA over the range of electric field strengths from 0 to 8 kV/cm. It can be concluded that the minimum electric field under atmospheric or vacuum conditions needed to levitate particles greater than approximately 10 μm in diameter in an electric field can be predicted well using Eq. (3).

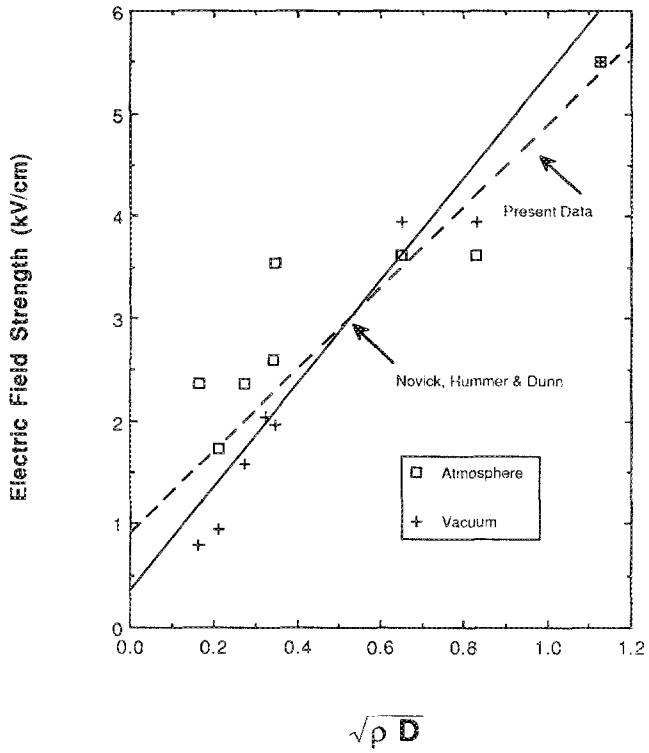

FIG. 3. Minimum electric field for particle levitation.

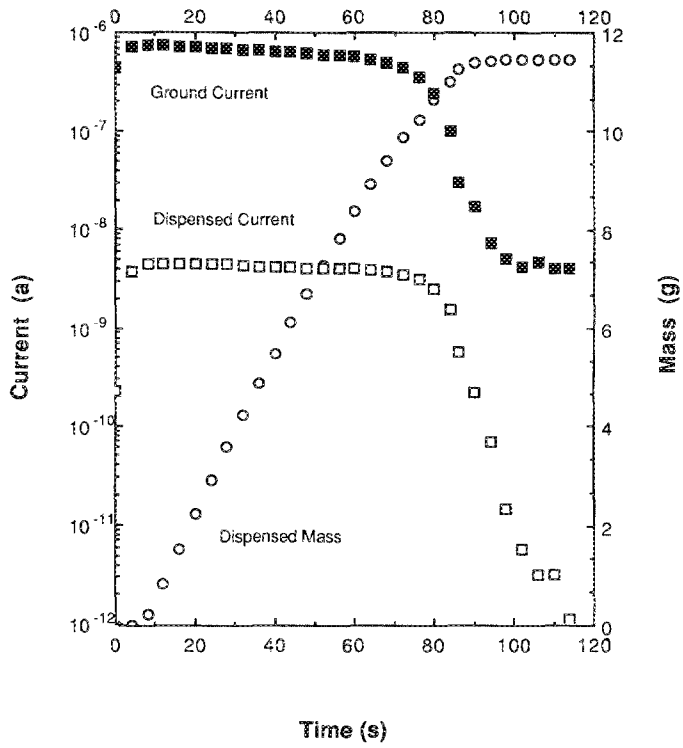

FIG. 4. Stainless-steel microsphere (Type 316) ground and dispensed particle currents and ejected mass (atmosphere, $E = 5.12$ kV/cm, $d = 2.54$ cm).

B. Dispensed mass flow rate

Another series of tests were performed using the materials listed in Table I to determine the dispensed mass flow rate as a function of the independent experimental variables. The dispensed mass flow rate is defined as the mass of powder emitted from the EPD per unit time. These tests were conducted in the open-air atmosphere so that the Sartorius balance could be used to acquire mass flow rate data. A typical result is shown in Fig. 4, where the accumulated mass of stainless-steel (Type 316) microspheres ejected from the EPD under atmospheric conditions is plotted versus time for the case of an interelectrode spacing of 2.54 cm and an electric field strength of 5.12 kV/cm. The results for all three types of particles tested at the four different interelectrode spacings were similar and showed that as the applied voltage increased for a particular interelectrode spacing (up to the point where arcing occurred between the electrodes) the dispensed particle mass flow rate also increased.

The mass flow rate of particles ejected from the EPD was found to depend upon particle density. For the two types of stainless-steel particles tested under the same operating conditions, the mass flow rates for the Type 410 particles with greater density (8000 kg/m^3) were approximately 10% greater than the Type 316 ones with lesser density (7700 kg/m^3). The results of the silver-coated microsphere tests further showed a more noticeable effect of particle density on the mass flow rate. Although the volumetric flow rate for the silver microspheres was greater than that for either of the stainless steel particle cases, its dispensed mass flow rate was an order of magnitude less. This was consistent with the difference in particle density between the two materials (850 vs 8000 kg/m^3 for the silver-coated and the Type 410 stainless-steel particles, respectively). The effects of voltage and interelectrode spacing, although evident, were not as prominent for the silver-coated microsphere test cases. This is probably because a much weaker electric field strength was required to levitate these particles as compared to the stainless steel particles.

The dispensed mass flow rate was found to depend also on the interelectrode spacing of the EPD. As the spacing was increased, the mass flow rate increased as well for the same electric field strength. The ejected stainless steel (Type 410) particle mass versus time is plotted as a function of the electric field strength in Fig. 5. For each of the three electric field strength cases on this plot, there are three distinct curves. The slopes of these curves represent the mass flow rates obtained at the different interelectrode spacings. The higher mass flow rates were obtained at the large interelectrode spacings for each of the electric field strength cases shown.

Ideally, for a parallel-plate capacitor arrangement, all curves of the mass flow data would collapse onto one curve for each electric field strength. It is postulated that this would not occur in these tests because of the nonuniform electrode geometry of the EPD. However, at the higher electric fields and larger interelectrode spacings, it can be seen that the data approach a limit that can be represented by one curve. This limit is presumed to occur when the electric field between electrodes becomes predominantly two dimensional. It is apparent that at the lowest interelectrode spacing, 1.27 cm, the nonuniform geometry of the upper and lower electrodes is such that this did not occur. However, as this interelectrode distance is increased, the nonuniform geome-

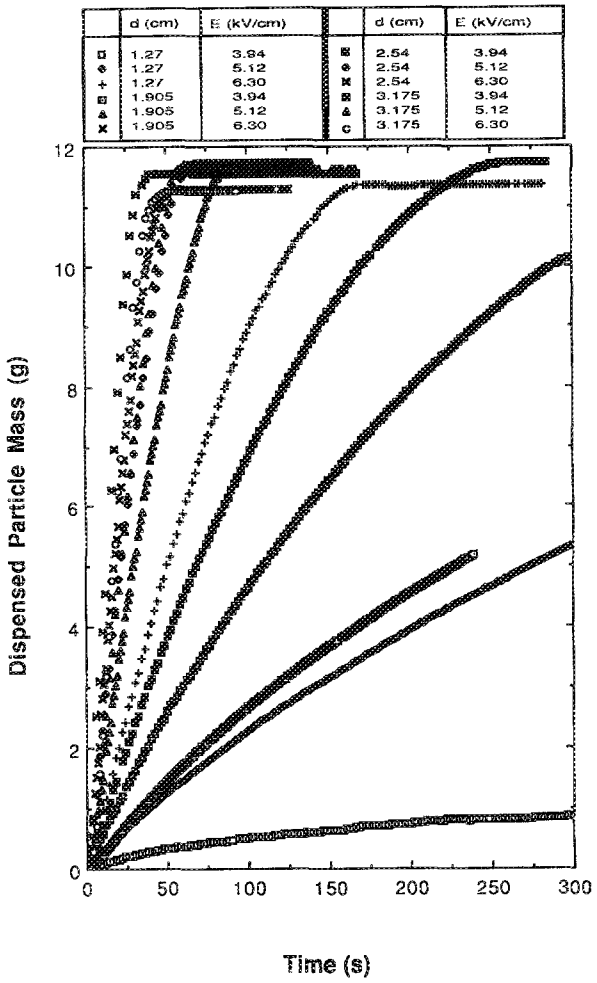

FIG. 5. Stainless-steel microsphere (Type 410) ejected mass for various electric field strengths (atmosphere).

try of the electrode becomes less important and apparently the electric field becomes more two dimensional.

These temporal measurements of the dispensed particle mass also could be correlated nondimensionally, independent of the particle type, interelectrode spacing and applied voltage. This was accomplished by postulating that the effluent mass flow rate was directly proportional to the particle mass present in the center electrode particle reservoir. This implied that the total particle mass accumulated on the copper collection plate below the EPD exit at any given time m_p was related to the final accumulated mass m_f by the expression

$$m_p/m_f = 1 - \exp(-t/\tau), \tag{14}$$

where τ is the time at which $1/e$ of the total particle mass has been collected on the plate. τ represents the physical time constant of this first-order system, which can be related to other experimental variables using Eq. (4):

$$\tau = 6m_i/\dot{n}\pi\rho D_{30}^3, \tag{15}$$

where m_i represents initial mass of paticles in the reservoir and $\dot{n}$ the particles per second leaving the reservoir. Since no model exists at present for predicting $\dot{n}$, each value of τ must be determined empirically. The acquired data expressed in this format are shown for the case of the stainless-steel (Type 410) particles in Fig. 6 for the three electric fields (3.94, 5.12, and 6.30 kV/cm) and two interelectrode spacings (1.27 and 2.54 cm) investigated. Although there is some minor variance in the data as the accumulated mass approaches the final mass, there is no consistent dependency on the electric field or interelectrode spacing. Similar results were obtained for the other two particle types examined.

Average mass flow rate data in all tests were obtained also to allow for comparison between the atmospheric and vacuum cases. The average mass flow rate for all tests was determined by dividing the total mass collected by the total dispensing time. From the results, for all three paticle cases under both atmospheric and vacuum conditions, the mass flow rate was found to be independent of the two pressures tested.

C. Particle current lost to ground

Measurements of the ground current were made using the materials listed in both Tables I and II; however, only those listed in Table I were tested extensively under both atmospheric and vacuum conditions for various interelectrode spacings. The ground current versus time for the case of the stainless-steel (Type 316) microspheres in atmosphere also is shown in Fig. 4. These results were typical of those obtained using the other particle types. They clearly revealed that as the electric field strength was increased, the current lost to ground increased significantly. This is attributed directly to the increase in charge on each particle [as shown by Eqs. (1), (5), and (8)] as well as to the increase in the number of particles that were oscillating inside the EPD,

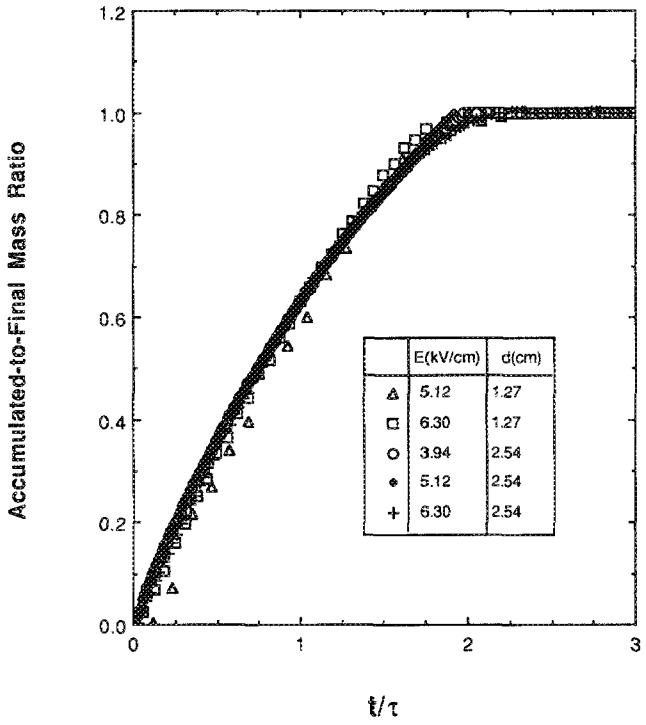

FIG. 6. Stainless-steel microsphere (Type 410) nondimensional ejected mass for various electric field strengths and electrode spacings (atmosphere).

which occurred as a result of the increase in mass flow rate with increasing electric field strength. For a given volume of powder, the EPD dispensed all of the supplied particles in less time as the applied voltage was increased. This implied that the mass flow rate increases as the voltage is increased (subject to arcing limitations). For the lowest applied voltage case examined (5.0 kV), the particle mass flow rate was low enough to achieve steady-state operation over a duration of approximately 35 s for 2 cm^3 of stainless-steel particles.

The effect of interelectrode spacing on the current lost to ground during EPD operation under atmospheric conditions was also investigated. The magnitude of the ground current for a constant electric field strength was found to increase with interelectrode spacing for all electric field cases examined. This effect can be explained by Eq. (8) only if the number of particles levitated per unit time increases with interelectrode spacing or if the number of bounces increases. Because the approximate percentage increase was the same as that percentage increase found for the mass flow rate (as the interelectrode spacing was increased while maintaining the same electric field strength), this behavior is consistent with the expectation that the ground current is directly proportional to the mass flow rate. It is also important to note that for a given amount of material, the duration of particle motion, as indicated by the ground current, was shorter for the 2.54 cm interelectrode spacing than for the 1.27 cm interelectrode spacing. This is a result of the mass flow rate being proportional to the interelectrode spacing for a similar electric field strength. Under vacuum conditions, this dependence on the interelectrode spacing was found to be similar. The most noticeable difference between the atmospheric and vacuum cases was that the magnitude of the ground current under vacuum conditions was greater for the same electric field strength and interelectrode spacing by approximately 150% to 200%. This is attributed to the presence of charge leakage that occurs under atmospheric conditions, as previously discussed.

The effect of particle material type on the ground current is best seen by examining the results of vacuum tests conducted using both the silver-coated and stainless-steel (Type 410) particles. These are shown in Figs. 7(a) and 7(b), respectively. These results reveal a significant effect of particle material type. The two most obvious differences in these results are the maximum amplitudes and durations of the ground currents. The silver-coated microspheres produced a ground current a full order of magnitude greater than the stainless steel particles. This was expected based on Eqs. (5) and (8), which predict that the ground current is inversely related to the material density. Because the silver-coated particles have approximately one-tenth the density of the stainless-steel particles, the duration of the ground current is expected to be greater than for the stainless steel particle case (with all other parameters equal in these experiments). However, compared to the stainless-steel case, the ground current resulting from the silver-coated particle "bounces" was significantly shorter, implying that the other parameters were not individually equal. Although the mass flow rate of the silver-coated particles was one-tenth that of the stainless-steel particles, their volumetric flow rate was

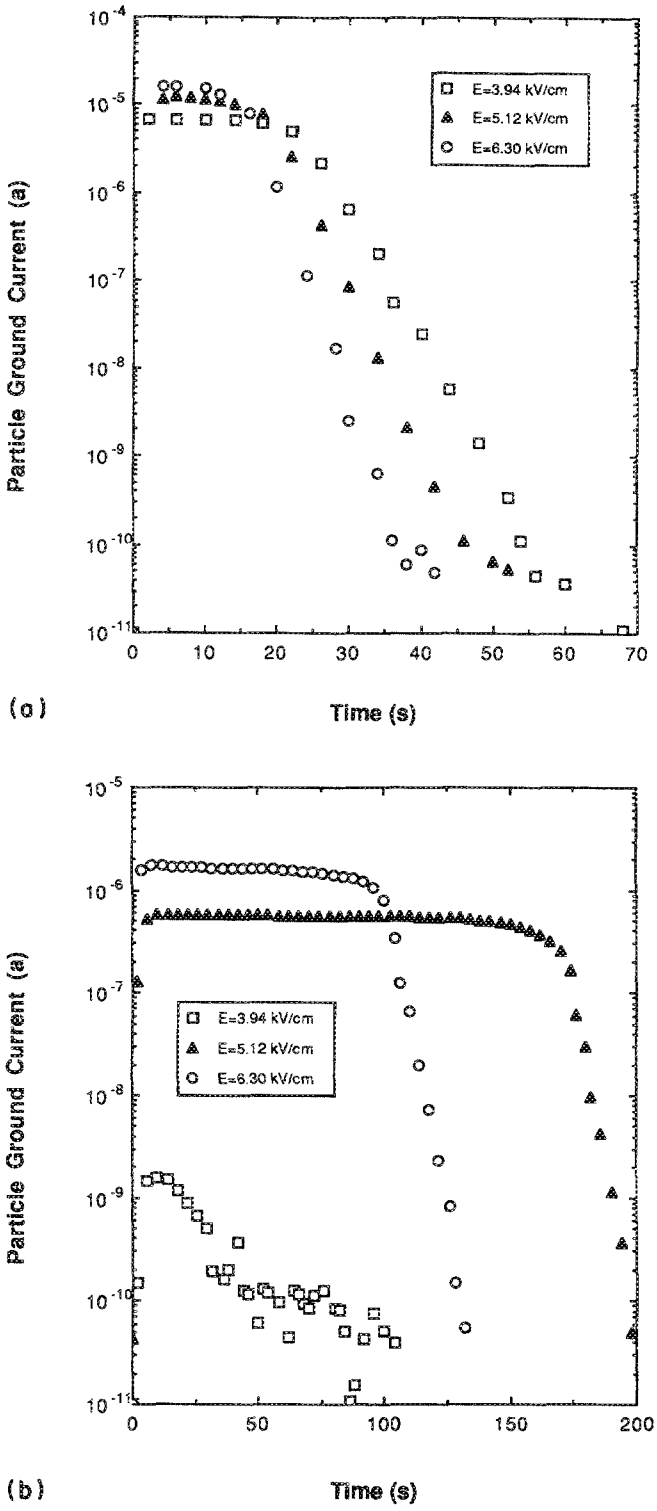

FIG. 7. (a) Silver-coated microsphere (Ag SF-14) ground current for various electric field strengths (vacuum, $d = 1.27$ cm). (b) Stainless-steel microsphere (Type 410) ground current for various electric field strengths (vacuum, $d = 1.27$ cm).

greater; hence, their number concentration inside the EPD was greater. For this reason, it took longer to dispense the stainless-steel particles, which resulted in a ground current that was less in magnitude but longer in duration. At present, it is clear that all individual parameters cannot be com-

pletely isolated for such experiments. Further work is required in this area before accurate operational predictions of the EPD can be made.

D. Dispensed particle current

Measurements of the dispensed particle current were made using most of the materials listed in both tables. The dispensed particle current is defined as the current carried by the particles emitted from the EPD. This current, as shown in Fig. 4 for stainless-steel (Type 316) microspheres emitted in atmosphere, follows trends similar to those of the ground current. The same trends were exhibited for other particle types tested under both atmospheric and vacuum conditions.

For those cases in which steady-state operation was achieved, it was possible to use single particle theory for both the atmospheric and vacuum cases to predict the measured average charge acquired by a particle, regardless of the material, electric field strength, or interelectrode spacing tested. The result of this comparison for the vacuum cases of six different particle types is shown in Fig. 8, in which the measured average charge per particle for a given electric field strength, interelectrode spacing, and known particle characteristics is plotted versus the value predicted using single particle theory. Here, the measured average charge acquired by a particle was determined by dividing the integral of the dispensed particle current over the dispensing time by the total number of particles found using Eq. (4). The theoretical values were determined using Eq. (6), where the particle diameters of average area and mass were those determined from the PDPA system measurements of their respective experimental cases. As shown in the figure, there is reasonable agreement between the measured and predicted values, especially for particle charge values above approximately $1\ E-14\ C$. For particle charges less than this value, the measured values approach an asymptotic limit equal to approximately $3\ E-16\ C$ as the particle charge decreases. This limit is the same order of magnitude as the contact potential charge cited by Cho[5] for a metal sphere in contact with a conducting plate. Using his approach, and assuming the distance between the sphere and the plate to be 0.01 μm and the intermolecular distance to be 1 μm, the capacitance between the particle and plate is $6.5\ E-16\ F$. This subsequently yields a contact potential ranging from approximately 0.65 to $6.5\ E-16\ C$ for work function values from 0.1 to 1.0 eV for the materials used in the present experiments.

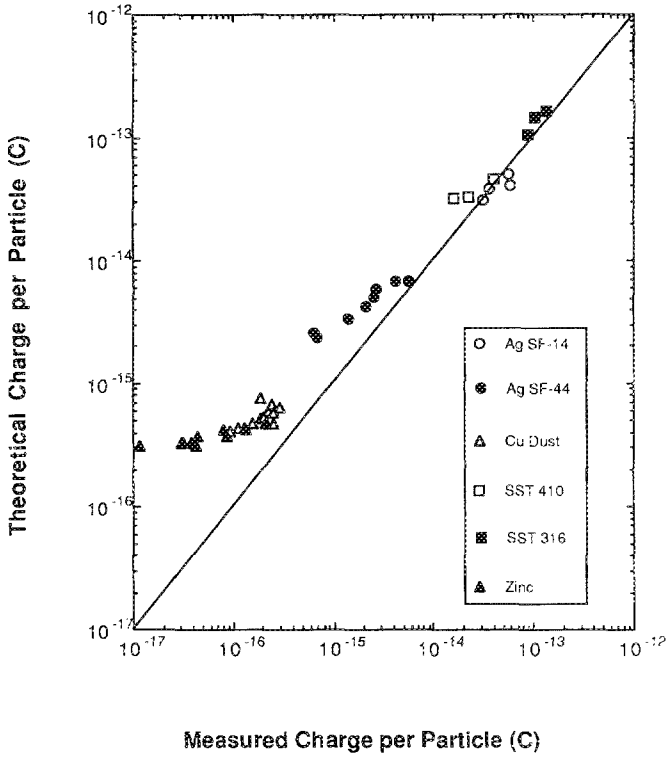

FIG. 8. Average charge per particle: theory vs experiment.

A similar comparison for the atmospheric cases revealed that the measured average charge acquired by a particle was approximately 50% less than its vacuum case counterpart. Similarly, the dispensed particle current was approximately 150%–200% less. Both these differences are attributed to the leakage of charge from the particle under atmospheric conditions, as discussed earlier.

In all cases examined, the dispensed particle current was measured to be two to three orders of magnitude less than the particle current lost to ground. For both types of stainless steel particles, the measured dispensed particle current was approximately two orders of magnitude less than the ground current; for the silver-coated particles it was approximately three orders of magnitude less. A typical comparison of the ground and dispensed particle currents measured versus time can be seen in Fig. 4. In this case, steady-state operation was achieved over the period from approximately 20 to 50 s. From single-particle theory, as given by Eq. (9), this implies that there were approximately one thousand particle-ground electrode collisions for a silver-coated particle before it exited the EPD. Along the same lines, there were approximately one hundred collisions for the stainless-steel particles. The calculated number of particle-ground electrode collisions also increased as the applied voltage was increased but these collisions occurred over a shorter period of time because of the fixed volume of particles used for each test.

E. Dispensed particle velocity

Measurements were made at 1.27 cm below the exit orifice of the EPD along its axial centerline of the average dispensed particle velocity of the materials listed in Table I under both atmospheric and vacuum conditions using the PDPA system and of those listed in Table II under vacuum conditions using the PSCV system.

The measurements conducted under atmospheric conditions for all three spherical particle types yielded average velocities that did not depend upon the electric field strength (i.e., upon both the applied voltage and the interelectrode spacing). These average velocities $\pm$ their standard deviations were 0.85 ± 0.10, 1.06 ± 0.09, and 0.62 ± 0.09 for the stainless-steel (Types 410 and 316) and the silver-coated particles, respectively. These results imply that under atmo-

spheric conditions each of the particle types reached an effective terminal velocity (subject to electrostatic and gravitational forces) at the point of measurement.

The measurements conducted under vacuum conditions for six of the particle types listed in the tables revealed average velocities that depended upon the material type, applied voltage, and interelectrode spacing. These measured average velocities are shown in Fig. 9. In this figure, the measured average velocity is plotted versus that calculated using Eq. (12), in which the particle charge is found from single particle theory using Eq. (6). It can be seen that the particles of relatively high density (Cu dust, stainless-steel, and zinc particles) have measured average velocities of approximately 2 m/s or less, whereas those of relatively low density (silver-coated microspheres) have velocities approximately 2 m/s or greater. These higher velocities for the lower density particles were the result primarily of the greater electrostatic contribution to the velocity, as given by the first term on the right-hand side of Eq. (12), which is inversely proportional to the material density. For these cases, the electrostatic contribution to the velocity, as determined using Eq. (12), was approximately ten times greater than its gravitational contribution. On the other hand, the contributions for the higher density materials were approximately equal. These results imply that reasonable agreement between experiment and theory can be achieved using single particle theory.

F. EPD dispensing efficiency

Additional experiments were performed to determine the dispensing efficiency of the materials listed in the tables as a function of the applied voltage, interelectrode spacing, and environmental pressure. Here, the dispensing efficiency of the EPD is defined as the ratio of the amount of powder dispensed m_f to the amount of powder supplied m_i. In these experiments, the EPD was operated until the dispensed particle current decreased more than two orders of magnitude below the initial current or to identified background levels. Some powder was not ejected due to particle adhesion to walls or collection in crevices inside the EPD. For all cases examined, this efficiency at a particular interelectrode spacing was found to increase with increasing electric field strength until essentially all of the particles were emitted. With all other conditions similar, there were no discernible differences between the atmospheric and vacuum cases for a particular type of particle.

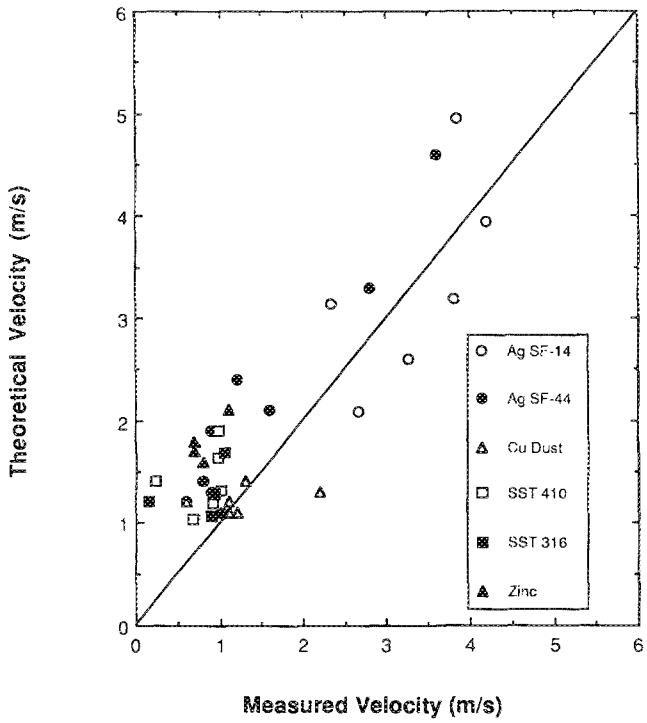

FIG. 9. Average dispensed centerline particle velocity for various material types (vacuum).

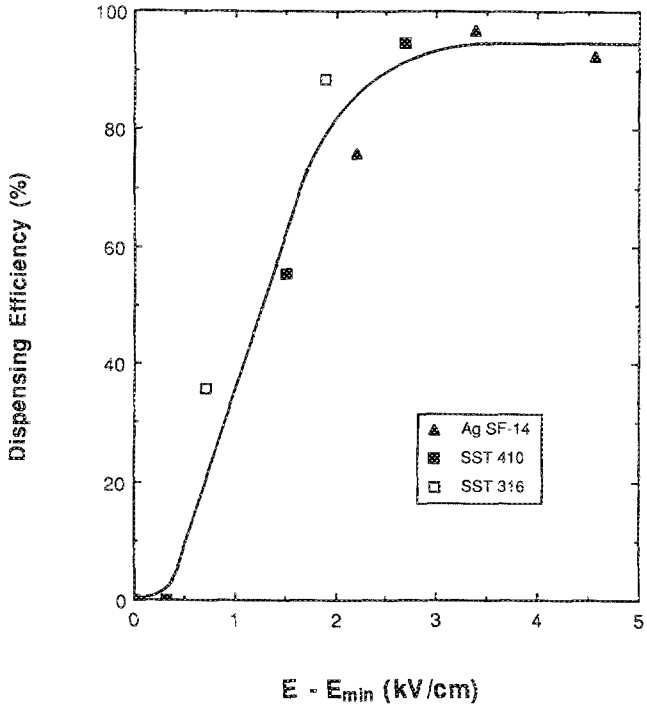

FIG. 10. EPD particle dispensing efficiency for various material types (atmosphere, $d = 1.27$ cm).

This efficiency, when expressed as a function of the strength of the electric field above the minimum field required for particle levitation, was found to be independent of particle type for all of the atmospheric cases. The results of the experiments conducted using the three particle types listed in Table I are displayed in Fig. 10 for the smallest of the four interelectrode spacings examined (1.27 cm), which includes all of the data obtained for that interelectrode spacing. It can be seen that the efficiency increases toward a maximum final value (95%) as the value of $E - E_{\min}$ increases, independent of particle type.

Further, it was found that as the interelectrode spacing was increased, the maximum efficiency was attained at a lower value of $E - E_{\min}$. At the largest interelectrode spacing examined (3.175 cm), the maximum efficiency was attained at an electric field strength slightly greater than that required for particle levitation. This effect of interelectrode spacing is illustrated in Fig. 11, in which the various efficien-

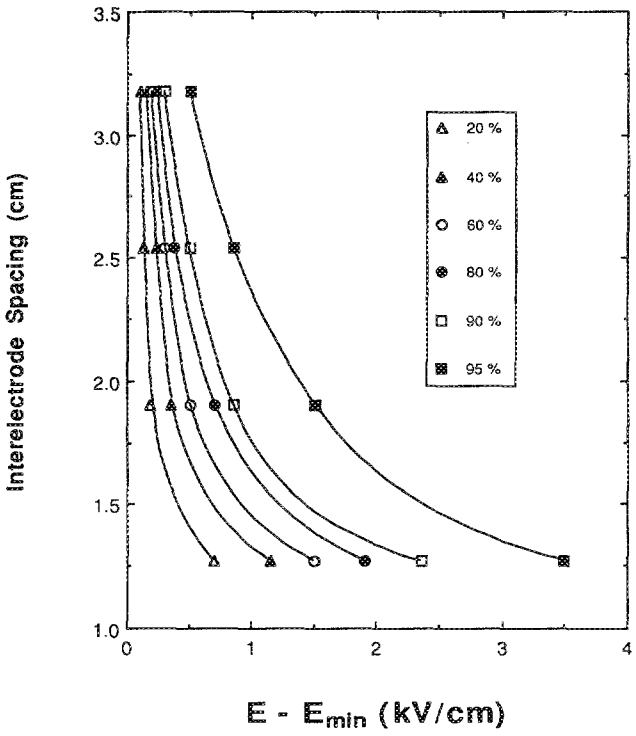

FIG. 11. EPD particle dispensing efficiencies for various interelectrode spacings (atmosphere).

cies achieved are plotted as a function of the interelectrode spacing and the electric field strength above the particle levitation minimum. The constant efficiency lines were obtained from a best fit of the data when plotted for each interelectrode spacing in the same manner as in Fig. 10. As shown in Fig. 11, very little electric field strength above the particle levitation minimum is required at the largest interelectrode spacing to achieve the maximum efficiency. This increased efficiency at large interelectrode spacings for a given electric field strength above minimum is postulated to be the consequence of a more two-dimensional electric field inside the EPD that probably is achieved at the larger interelectrode spacings, as discussed previously.

It should be noted, however, that under certain circumstances the EPD dispensing efficiency can depend upon the material type. This has been demonstrated by Olansen.[12] In particular, the EPD cannot efficiently dispense insulating particles in a vacuum (because there is no medium for charge transfer) or particles less than approximately 10 μm in diameter (because particle adhesion is dominant).

V. SUMMARY

In this study, the operational performance of an electrostatic particle dispensing device was determined under different operating conditions based upon four independent variables. These were the environmental pressure in which the dispenser was operated, its interelectrode spacing and applied voltage, and the type of particle used.

In order for particles to be dispensed from the EPD, a minimum applied electric field strength was necessary to initially levitate the particles from the center electrode. This minimum electric field strength was found to depend upon the diameter and density of the particles used and could be predicted using the theory presented herein.

The dispensed particle mass flow rate, dispensed particle current, and particle current lost to ground were found to depend on the magnitude of the electric field strength, interelectrode spacing, and density of the particles used. The temporal measurements of the dispensed particle mass also could be correlated nondimensionally, independent of the paticle type, interelectrode spacing, and applied voltage. As a result of the numerous particle–electrode collisions that occurred inside the EPD, it was determined that the measured particle ground current was approximately two to three orders of magnitude greater than the dispensed particle current. The measured average charge acquired by a particle as determined from the dispensed particle current could be predicted using the theory presented.

The dispensed average particle velocity measured under atmospheric conditions was found to be independent upon the applied voltage and interelectrode spacing, whereas under vacuum conditions it was not. Under vacuum conditions, greater velocities were achieved using relatively low density particles which was the consequence of a significant electrostatic contribution to particle acceleration. These measured average velocities could be predicted using the theory presented.

The dispensing efficiency of the EPD was found to depend upon the electric field and type of particles used. This efficiency, when expressed as a function of the strength of the internal electric field above the minimum field required for particle levitation against gravity, was shown to be indepenent of particle type for all of the atmospheric cases investigated.

In conclusion, the results of this study collectively support that it is possible to dispense micrometer-size particles under both atmospheric and vacuum conditions using an electrostatic device that is mechanically simple and does not rely upon the use of a carrier gas.

ACKNOWLEDGMENTS

This work was performed under MIPR No. FY76168800343 between the University of Chicago and the Department of Defense and under Contract No. 62622401 between Argonne National Laboratory and the University of Notre Dame. The authors would like to thank P. Higgins, R. Haglund, M. Sanchez, D. Larson, and W. Clark for conducting some of the experiments reported herein, R. Macedo for helping construct the vacuum facility, designing the EPD, and overseeing its fabrication, T. Dickman for machining several critical parts, and P. A. Industries Inc. (Chattanooga, TN) for supplying samples of several powders used in these experiments.

[1]T. U. Yu and G. M. Colver, IEEE Trans. Ind. Appl. IA-23, 127 (1987).
[2]H. Shelton, C. D. Hendricks, and R. F. Wuerker, J. Appl. Phys. 31, 1243 (1960).
[3]P. Benjamin, *A History of Electricity* (Wiley, New York, 1985).

[4]B. Franklin, *Experiments and Observations on Electricity Made at Philadelphia in America, by Mr. Benjamin Franklin, and Communicated in Several Letters to Mr. P. Collison, of London, F.R.S. London* (Printed and sold by E. Crave at St. John's Gate, 1751).
[5]A. Y. H. Cho, J. Appl. Phys. **35**, 2561 (1964).
[6]G. M. Colver, J. Appl. Phys. **47**, 4839 (1976).
[7]O. A. Myazdrikov and V. N. Puzanov, Zavod. Lab. **35**, 1265 (1969).
[8]D. W. Cooper, H. L. Wolfe, and R. J. Miller, presented at the Fine Particle Society 17th Annual Meeting, San Francisco, CA, 1986.
[9]D. W. Cooper and H. L. Wolfe, IBM Res. Rept., Project No. 60249 (1988).
[10]V. J. Novick, C. R. Hummer, and P. F. Dunn, J. Appl. Phys. **65**, 3242 (1989).
[11]R. C. Adamo and J. E. Nanevicz, Stanford Research Institute Report, Project No. 3599, 1975.
[12]J. B. Olansen, M. S. thesis, University of Notre Dame, 1988.
[13]W. D. Bachalo and M. J. Houser, Opt. Eng. **23**, 583 (1984).
[14]D. J. Holve and K. Annen, Opt. Eng. **23**, 591 (1984).